Exact dynamics of interacting qubits in a thermal environment: results beyond the weak coupling limit

2013 New J. Phys. 15 023044

(http://iopscience.iop.org/1367-2630/15/2/023044)

New Journal of Physics
The open access journal for physics

Exact dynamics of interacting qubits in a thermal environment: results beyond the weak coupling limit

Lian-Ao Wu[1], **Claire X Yu**[2] **and Dvira Segal**[2,3]

[1] Department of Theoretical Physics and History of Science, The Basque Country University (EHU/UPV) and IKERBASQUE—Basque Foundation for Science, E-48011 Bilbao, Spain

[2] Chemical Physics Theory Group, Department of Chemistry and Centre for Quantum Information and Quantum Control, University of Toronto, 80 St George Street, Toronto, Ontario M5S 3H6, Canada

E-mail: dsegal@chem.utoronto.ca

New Journal of Physics **15** (2013) 023044 (18pp)
Received 19 November 2012
Published 27 February 2013
Online at http://www.njp.org/
doi:10.1088/1367-2630/15/2/023044

Abstract. We demonstrate an exact mapping of a class of models of two interacting qubits in thermal reservoirs to two separate problems of spin–boson-type systems. Based on this mapping, exact numerical simulations of the qubits dynamics can be performed, beyond the weak system–bath coupling limit and the Markovian approximation. Given the time evolution of the system population and coherences, we study as an application the dynamics of entanglement between the pair of qubits immersed in boson thermal baths, showing a rich phenomenology, including an intermediate oscillatory behavior, the entanglement sudden birth, sudden death and revival. We find that the occurrence of entanglement sudden death in this model depends on the portion of the zero and double excitation states in the subsystem initial state. In the long-time limit, analytic expressions are presented at weak system–bath coupling, for a range of relevant qubit parameters.

[3] Author to whom any correspondence should be addressed.

Contents

1. Introduction

Understanding the dynamics of a dissipative quantum system is a prominent challenge in physics, as a quantum system is never perfectly isolated from a larger environment. A minimal, yet highly rich model for exploring quantum dissipation effects, is the spin–boson model, including an impurity two-level system (referred to as a spin) coupled to a thermal reservoir. This model displays a rich phase diagram in the equilibrium regime [1, 2]. The nonequilibrium version of this model, referring to the case where the spin is coupled to two thermal reservoirs, has been suggested as a toy model for exploring quantum transport phenomenology through an anharmonic nanojunction [3, 4]. In this case, the generic situation is that of a nonequilibrium steady state, regardless of the initial preparation.

Interacting two-level systems are the basic element in quantum computation; thus it is paramount to extend the minimal spin–boson scenario and describe more complex modular systems, e.g. two interacting qubits immersed in a thermal environment [5, 6]. For a schematic representation, see figure 1. The qubits may share their thermal environment, or may separately couple to independent baths, prepared at a nonzero temperature. The latter situation corresponds to the case where the qubits are not necessarily placed close to each other. In another relevant setup, one qubit couples indirectly to a thermal reservoir, through its interaction with the other qubit. This situation effectively corresponds to a subsystem anharmonically coupled to a harmonic bath, allowing one to introduce nontrivial nonlinear effects [7]. In such systems one should consider (at least) four energy scales: the internal qubit energetics, controlling its isolated (Rabi oscillation) dynamics, qubit–bath interaction strength and the environment temperature, leading to decoherence and relaxation processes; and qubit–qubit coupling energy, admitting state transfer between qubits and a nontrivial gate functionality. Physical realizations include ultracold atoms in optical lattices [8], trapped ions [9], resonator-coupled superconducting qubit arrays [10–13] and electron spins in quantum dots and doped semiconductors [5, 14]. In particular, in a recent experiment Schulman *et al* [15] have demonstrated entanglement between electrostatically coupled qubits realized by quantum dots in a semiconductor heterostructure.

The dissipative multi-qubit system recently served as a simple model for resolving issues related to coherence dynamics in the time evolution of biological molecules, e.g. the Fenna–Matthews–Olson complex [16, 17]. In these studies, a chromophore in a complex biomolecular system is represented by a qubit, and electronic energy exchange between chromophores is realized by including qubit–qubit direct coupling energies in the Hamiltonian [18–24].

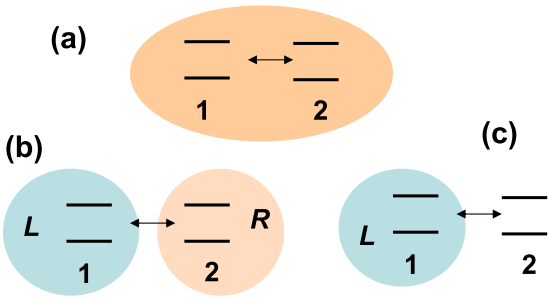

Figure 1. Scheme of the model system including two interacting qubits (a) immersed in a common bath, (b) coupled to separate baths, L and R, and (c) with qubit '2' coupled to a thermal bath only through its interaction with qubit '1'. This model can represent the nonlinear coupling of qubit '2' to a structured bath. Simulations were performed here assuming scenario (c).

The interaction of the chromophores with the environment, the solvent or the vibrational modes of the protein provides a dephasing mechanism. Efforts in this direction were focused on the identification of decoherence, relaxation and disentanglement timescales at low and high (ambient) temperatures. It should be noted that in these studies an isotropic exchange interaction was typically assumed [19], allowing one to immediately separate the dynamics of the single-excitation states from the zero and the doubly excited states. The implications of this setup (which is generalized here) are detailed in section 2.

Entanglement is associated with nonclassical correlations between two or more quantum systems [25]. Since it is a basic resource in quantum computation and information technology, it is important to understand the extent to which environmental-induced decoherence processes degrade and destroy it [26], or alternatively, generate [27–29] and maintain it [30]. It has recently been shown that two qubits in separate reservoirs may disentangle *at finite times*, as opposed to the behavior of coherences. This process is referred to as 'entanglement sudden death' [26, 31]. More recent theoretical and experimental studies have looked at related effects, e.g. the collapse and subsequent revival of the entanglement [32], or its delayed-sudden birth, induced by a dissipative bath [33]. Steady-state entanglement generation by dissipation has recently been observed in atomic ensembles [34]. These studies have assumed noninteracting qubits, and the system dynamics has been typically followed within quantum master equation approaches (the Redfield equation or Lindblad formalism [35]), by invoking the weak system–bath coupling approximation. The Markovian limit has been further assumed in many cases, see, e.g., [28, 36]. Non-Markovian dynamics was considered in, e.g., [37].

Dephasing dynamics in two-qubit systems has thus been studied in different contexts, adopting a variant of the two-qubit model. We can essentially organize those studies into two groups: in the first generic setup, the qubits do not directly interact, but they are initially entangled [26, 27, 31–33, 37]. In this scenario the fundamental question is the survival (and death) of entanglement. This picture is particularly interesting for potential applications in quantum information science, for example in quantum cryptography [38]. The second setup incorporates a direct exchange interaction between the qubits which may be stationary or time dependent [5, 39–42]. This situation is more relevant for quantum computing applications, for implementing quantum gates [5] and for modeling the energy transfer in biomolecules [19].

Our work here corresponds to the second scenario, which is generalized here by building an anisotropic *XYZ* qubit–qubit direct interaction form.

In this work, we analytically demonstrate that a class of interacting two-qubit systems dephased by separate thermal reservoirs or by a common bath can be mapped onto two uncoupled problems of a spin coupled to a thermal environment, allowing for an exact numerical solution of the qubits dynamics. For a bosonic environment and a particular system–bath interaction form, we perform those simulations using an exact numerical technique, the quasi-adiabatic path-integral (QUAPI) approach [43, 44], providing the population and coherence dynamics of the system. With this at hand, we can follow the exact dynamics of entanglement between the qubits, as quantified by Wootters' concurrence [45]. For a range of system and bath parameters, analytic results are presented for describing the system behavior in the long-time limit.

Our contribution is twofold. Firstly, we show how the dynamics can be followed within a simple construction: while we take into account the zero excitation and double excitation states, under certain initial conditions their dynamics can be separated from the evolution of the single-excitation states. However, their contribution to the pair entanglement is paramount. Secondly, assuming a class of initial states, we study the qubits dynamics using a numerically exact method without further approximations. The results are valid beyond the weak system–bath coupling scenario, accommodating non-Markovian effects.

Our calculations display rich dynamics, including (temporal) population inversion between the zero excited and the doubly excited states. Particularly, inspecting the qubits entanglement, we observe the development of a *stationary* concurrence due to the coupling of the qubits to thermal baths. This result stands in direct contrast to the oscillatory behavior observed in the fully coherent regime. It demonstrates that while entanglement inherently relies on the existence of quantum correlations in the system, it nevertheless requires nonvanishing decoherence and relaxation effects in order to be stabilized and become useful for quantum technologies. Other phenomena detected and explained here are entanglement delayed sudden birth, sudden death and revival. These effects have been observed before in related models. However, as we obtain those characteristics within an exact numerical method, our treatment could be used to test approximation schemes.

The paper is organized as follows. In section 2, we describe the model of interest, and explain its mapping onto two separate spin–boson-type problems. In section 3, we explain how we follow the system dynamics, and include relevant expressions for calculating the qubits concurrence. Numerical results within QUAPI are included in section 4. The long-time limit of the qubits occupation, coherence and concurrence is discussed in section 5. Section 6 presents the conclusion. For simplicity, we use the conventions $\hbar \equiv 1$ and the Boltzmann constant $k_{\rm B} = 1$.

2. The model

The general model that is considered here includes two interacting qubits, $i = 1, 2$, immersed within separate reservoirs, L and R, respectively. The formalism can be reduced to describe a single-bath scenario. The total Hamiltonian includes three terms,

$$H = H_{\rm S} + H_{\rm B} + V_{\rm SB}. \tag{1}$$

where $H_{\rm S}$ and $H_{\rm B} = H_L + \mathrm{H}_R$ stand for the system and reservoirs Hamiltonians, respectively. The former includes the qubits with the internal energy bias ϵ_i and a qubit–qubit interaction

term V_{ss},

$$H_S = \epsilon_1 \sigma_1^z + \epsilon_2 \sigma_2^z + V_{ss},$$
$$V_{ss} = \frac{J}{2}[(1+\gamma)\sigma_1^x \sigma_2^x + (1-\gamma)\sigma_1^y \sigma_2^y + 2\delta \sigma_1^z \sigma_2^z]. \quad (2)$$

σ_i^p $(p = x, y, z)$ are the Pauli matrices for the ith spin, J is an energy parameter characterizing the exchange interaction, and γ and δ set the interaction anisotropy. Our mapping holds for a dephasing-type system–bath interaction model

$$V_{SB} = \sigma_1^z B_L + \sigma_2^z B_R. \quad (3)$$

Here, B_ν is a $\nu = L, R$ bath operator, with B_L coupled to spin '1' and B_R coupled to spin '2'. In the absence of qubit–qubit direct interaction, the dephasing dynamics of each qubit can be analytically obtained by using the small polaron transformation [46, 47]. Our study here is focused on an extension of this model for describing the dephasing dynamics of a dimer. A more general description would further involve bath-induced spin–flip processes, excluded here. Our modeling can thus be applied to situations that are approximated by a phase–loss interaction as in equation (3). For example, it is useful in describing excitonic energy transfer between chromophores in light harvesting biomolecules [18–20, 23, 24]. An effective (spin–boson) Hamiltonian is reached here based on the role of the medium electronic polarization in charge or energy transfer processes, between the subsystem states. We model each chromophore as a point dipole, and assume that the (polar) environment has a static-uniform dielectric constant. Each dipole polarizes the medium around it, and these induced electric fields act back on the dipoles, affecting the rate of energy transfer. These fields are next quantized, to be described by a collection of harmonic modes that are coupled through σ^z, the dipole polarization, to the chromophores.

From a different direction, the modeling (1)–(3) is also relevant in the area of quantum information processing when realizing qubits based on either charge or phase (flux) degrees of freedom in Josephson tunneling junctions. The qubits' parameters can be controlled by applying gate voltages and magnetic fields, and superpositions of different states have been observed using both flux and charge qubits [10, 11]. However, control resistive elements in the circuit produce voltage and current noise that cannot be entirely suppressed. These (thermal) fluctuations can be handled by (linearly) coupling the qubits to a harmonic environment with a suitable frequency spectrum. For charge qubits, fluctuations in the gate voltage circuit couple to σ^z [12]. To become practical in information processing applications, one needs to minimize both dephasing and environmental induced relaxation processes in such devices. In the regime where dephasing rate is much faster than population relaxation rate, when internal tunneling elements in each qubit are weak relative to the coupling to the bath, our model could serve in estimating the population, coherence and entanglement dynamics in these devices.

Our model includes XYZ qubit–qubit interactions. When $\gamma = 0$ the number operator of excitations in the system, $N = \sigma_1^z + \sigma_2^z + 2$, commutes with the Hamiltonian, $[N, H] = 0$. Thus, the total number of excitations is a constant of motion and the dynamics can be recovered by considering separately the behavior of each excitation number. However, when $\gamma \neq 0$ this commutator does not vanish, $[H, N] \neq 0$, and in principle the dynamics of the three excitation states (zero, single and double occupied) is coupled. In section 3 we show that for a class of direct-sum initial conditions the dynamics under nonzero γ can still be carried out in two separate branches.

In our simulations below, we adopt bosonic reservoirs: each thermal bath includes a collection of independent harmonic oscillators,

$$H_\nu = \sum_{k\in\nu} \omega_k a_k^\dagger a_k. \tag{4}$$

The operators $a_k^\dagger$ and a_k are bosonic creation and annihilation operators, respectively, ω_k is the mode frequency. We also assume that the interaction operators constitute the reservoirs displacements from equilibrium,

$$B_\nu = \sum_{k\in\nu} \lambda_k^{(\nu)} (a_k^\dagger + a_k). \tag{5}$$

Here, λ_k are system–bath coupling constants. However, the mapping described next, from the Hamiltonian (1) onto two spin–boson-type problems, neither relies on a particular bath statistics nor on the details of the operators B_ν. For example, it is valid for a model of two qubits in fermionic or spin environments. The Hamiltonian introduced so far takes into account two independent reservoirs. We could explore a similar setup with one qubit coupled to a thermal reservoir indirectly, through its interaction with the second qubit, mimicking nonlinear effects [7], see figure 1. Another relevant setup includes two qubits immersed in a common thermal reservoir.

The Hilbert space of the qubits is spanned by four vectors, $|00\rangle$, $|01\rangle$, $|10\rangle$, $|11\rangle$, forming the excitation basis of the Hamiltonian, where the left (right) digit indicates the state of qubit 1 (2). We now show that the Hamiltonian can be mapped onto two spin–boson-type models. We begin by defining four composite system operators,

$$\begin{aligned} P_z &= \tfrac{1}{2}(\sigma_1^z - \sigma_2^z), \quad Q_z = \tfrac{1}{2}(\sigma_1^z + \sigma_2^z), \\ P_x &= \tfrac{1}{2}\left(\sigma_1^x\sigma_2^x + \sigma_1^y\sigma_2^y\right), \quad Q_x = \tfrac{1}{2}\left(\sigma_1^x\sigma_2^x - \sigma_1^y\sigma_2^y\right). \end{aligned} \tag{6}$$

In the excitation basis, these operators take the explicit form

$$\begin{aligned} P_x &= |01\rangle\langle 01| + |10\rangle\langle 10|, \quad P_z = |10\rangle\langle 01| - |01\rangle\langle 10|, \\ Q_x &= |00\rangle\langle 11| + |11\rangle\langle 00|, \quad Q_z = |00\rangle\langle 00| - |11\rangle\langle 11|. \end{aligned} \tag{7}$$

Additionally, we construct two identity-type operators,

$$\begin{aligned} I_P &= |10\rangle\langle 01| + |01\rangle\langle 10|, \\ I_Q &= |00\rangle\langle 00| + |11\rangle\langle 11|. \end{aligned} \tag{8}$$

With these at hand, the Hamiltonian (1) can be written as

$$H = H_Q + H_P, \tag{9}$$

where

$$\begin{aligned} H_Q &= \epsilon Q_z + J\gamma Q_x + Q_z B + J\delta I_Q + H_B I_Q, \\ H_P &= \bar{\epsilon} P_z + J P_x + P_z \overline{B} - J\delta I_P + H_{\mathrm{B}} I_P. \end{aligned} \tag{10}$$

Here, $\epsilon = \epsilon_1 + \epsilon_2$, $\bar{\epsilon} = \epsilon_1 - \epsilon_2$, $B = B_L + B_R$ and $\overline{B} = B_L - B_R$. One can easily show that the following commutators vanish [48] ($m, n = x, z$):

$$[Q_m, P_n] = [P_m, \sigma_1^z\sigma_2^z] = [Q_m, \sigma_1^z\sigma_2^z] = 0. \tag{11}$$

The Hilbert space of two qubits can thus be factored into two direct-sum subspaces: the first, P, is spanned by $|01\rangle$ and $|10\rangle$. The second, Q, is spanned by $|00\rangle$ and $|11\rangle$. One can further prove

that P_x, $[P_x, P_z]$ and P_z generate an $SU^P(2)$ group, and Q_x, $[Q_x, Q_z]$ and Q_z generate another $SU^Q(2)$ group. The two groups have a direct-sum structure, $SU^P(2) \oplus SU^Q(2)$. We now note that P_x and P_z in subspace P play the role of the Pauli matrices σ^x and σ^z (in the space spanned by $|0\rangle$ and $|1\rangle$). The same principle holds for Q_x and Q_z in the Q subspace. Overall, in mapping equation (1) onto equation (10), we replaced a model of two interacting spins coupled each to its own thermal reservoir, by a model of two separate spin–boson-type systems, where each spin in the new model is coupled to *both* reservoirs.

The mapping described here holds for general reservoirs and a bilinear system–bath interaction form, with an arbitrary bath operator coupled to the subsystem. The results hold also when we apply a dressing transformation [49] W, $H' = W^\dagger H W$, on the two-qubits Hamiltonian, or the reservoirs. For example, we may introduce a spin–orbital coupling into V_{ss} via $W = \exp(\mathrm{i}\frac{\theta}{2}\sigma_1^z)$, while keeping the other terms in the total Hamiltonian unchanged:

$$V'_{ss} = \cos\theta V_{ss} + \sin\theta \frac{J}{2}[(1+\gamma)\sigma_1^y\sigma_2^x - (1-\gamma)\sigma_1^x\sigma_2^y]. \tag{12}$$

Another relevant case that can be simulated exactly relies on the absence of external fields, $\epsilon_1 = \epsilon_2 = 0$, taking $W = \exp(\mathrm{i}\frac{\pi}{4}(\sigma_1^y + \sigma_2^y))$. This results in

$$H'_S = \frac{J}{2}[(1+\gamma)\sigma_1^z\sigma_2^z + (1-\gamma)\sigma_1^y\sigma_2^y + 2\delta\sigma_1^x\sigma_2^x] \tag{13}$$

with $V'_{SB} = \sigma_1^x B_L + \sigma_2^x B_R$. After this transformation, the model has turned into the anisotropic XYZ-type model with flip–flop (σ_x) coupling between the system and reservoirs. In this form, the model describes energy exchange between the qubits and the baths, unlike the original Hamiltonian (equation (3)) which delineates dephasing effects. When $1-\gamma = 2\delta$, it reduces to the standard XY model, $H'_S = \frac{J}{2}[(1-\gamma)(\sigma_1^y\sigma_2^y + \sigma_1^x\sigma_2^x) + (1+\gamma)\sigma_1^z\sigma_2^z]$.

3. Dynamics and quantum entanglement

We explain here how we time evolve the reduced density matrix, to obtain the qubits dynamics. As the initial condition we consider a system–bath product state, where the reservoirs are prepared in a canonical–thermal state with an inverse temperature $\beta_\nu = 1/T_\nu$, $\rho_\nu = \mathrm{e}^{-\beta_\nu H_\nu}/Z_\nu$, $Z_\nu = \mathrm{Tr}_B[\mathrm{e}^{-\beta_\nu H_\nu}]$ is the partition function. In order to separate the dynamics into the Q and P branches, we must adopt a direct sum Q–P initial state for the qubits. Overall, the total density matrix at time $t = 0$ must be written as

$$\rho(0) = \begin{pmatrix} \rho_P(0) & 0 \\ 0 & \rho_Q(0) \end{pmatrix} \otimes \rho_B. \tag{14}$$

For a particular example, see equation (23). Special initial states can be prepared within Josephson junction qubits, by tuning the gate voltage and magnetic fields [11]. In photosynthetic systems, initial conditions were typically taken to include only the single excitation states [19–24]. Under this construction, the reduced density matrix follows

$$\begin{aligned} \rho_S(t) &= \mathrm{Tr}_B[U(t)\rho(0)U^\dagger(t)] \\ &= \mathrm{Tr}_B \begin{pmatrix} U_P(t)\rho_P(0)\rho_B U_P^\dagger(t) & 0 \\ 0 & U_Q(t)\rho_Q(0)\rho_B U_Q^\dagger(t) \end{pmatrix}. \end{aligned} \tag{15}$$

The trace is performed over the L and R degrees of freedom. The time evolution operators, $U(t) = U_Q(t) \oplus U_P(t)$, are defined as

$$U_Q(t) = \mathrm{e}^{-\mathrm{i}tH_Q}, \quad U_P(t) = \mathrm{e}^{-\mathrm{i}tH_P}, \tag{16}$$

with H_P and H_Q given in equation (10). Equation (15) establishes an important result: the dynamics of the two-qubit system proceeds in two independent branches, each equivalent to a model of a spin coupled to thermal reservoirs. In the case of bosonic baths, the dynamics in each branch is followed next using the QUAPI technique [43], a numerically exact simulation tool that can be easily extended to include more than one thermal reservoir. The specific QUAPI implementation follows [44]. The output of this calculation is the reduced density matrix of the qubits. We use this information and investigate the time evolution of entanglement between the qubits. As a side comment, we note that if the two qubits identically couple to a common bath, $B_L = \sum_{k\in L} \lambda_k^{(L)}(a_k^\dagger + a_k)$ and $B_R = \sum_{k\in R} \lambda_k^{(R)}(a_k^\dagger + a_k)$ with $\lambda_k^{(L)} = \lambda_k^{(R)}$ for all the modes, then $\bar{B} = 0$. As a result, only the Q subspace becomes susceptible to decohering effects, while the P subspace becomes an invariant subspace or a 'decoherence-free' subspace.

Based on equations (14)–(16), we conclude that the reduced density matrix ρ_S is the so-called 'X state' [50, 51] at all times, once we organize it in the standard order of basis vectors $|00\rangle$, $|01\rangle$, $|10\rangle$ and $|11\rangle$,

$$\rho_S = \begin{pmatrix} (\rho_S)_{00,00} & 0 & 0 & (\rho_S)_{00,11} \\ 0 & (\rho_S)_{01,01} & (\rho_S)_{01,10} & 0 \\ 0 & (\rho_S)_{10,01} & (\rho_S)_{10,10} & 0 \\ (\rho_S)_{11,00} & 0 & 0 & (\rho_S)_{11,11} \end{pmatrix}. \tag{17}$$

This is the main result of this paper: with certain initial conditions, the dynamics of a class of dissipative interacting qubits (equations (1)–(3)) can be reached via the solution of two spin–boson-type problems, and the reduced density matrix satisfies the form (17) at all times. It should be noted that the dynamics of a system with initial coherences between the Q and P branches could in principle be solved in a numerically exact way using a four-state subsystem within QUAPI, resulting in a full matrix instead of the X form (17).

Different quantities are of interest, e.g. the timescale for maintaining coherences in the system [23]. Here, we focus on the behavior of quantum correlations in the system [25], computed next in a numerically exact way beyond weak coupling. In particular, we quantify the degree of entanglement between the qubits using Wootters' concurrence [45]. For mixed states it is calculated by considering the eigenvalues of the matrix $r(t) = \rho_S(t)\sigma_1^y \otimes \sigma_2^y \rho_S^*(t)\sigma_1^y \otimes \sigma_2^y$, given here by

$$\lambda_{1,2} = \left[\sqrt{(\rho_S)_{01,01}(\rho_S)_{10,10}} \pm |(\rho_S)_{01,10}|\right]^2,$$
$$\lambda_{3,4} = \left[\sqrt{(\rho_S)_{00,00}(\rho_S)_{11,11}} \pm |(\rho_S)_{00,11}|\right]^2. \tag{18}$$

In terms of these eigenvalues (not ordered), the concurrence is defined as [45]

$$C(t) = \max(2\max(\sqrt{\lambda_1}, \sqrt{\lambda_2}, \sqrt{\lambda_3}, \sqrt{\lambda_4}), -\sqrt{\lambda_1} - \sqrt{\lambda_2} - \sqrt{\lambda_3} - \sqrt{\lambda_4}, 0). \tag{19}$$

It varies from $C = 0$ for a disentangled state to $C = 1$ for a maximally entangled state. In the present case it reduces to

$$C(t) = \max(0, 2F_1, 2F_2) \tag{20}$$

with

$$F_1 = |(\rho_S)_{01,10}| - [(\rho_S)_{00,00}(\rho_S)_{11,11}]^{1/2},$$
$$F_2 = |(\rho_S)_{00,11}| - [(\rho_S)_{01,01}(\rho_S)_{10,10}]^{1/2}. \tag{21}$$

The dynamics of concurrence for an X-state density matrix has been examined in different works. For example, in [36] it is demonstrated that the effect of entanglement sudden death should always take place in a noninteracting qubit system once coupled to a finite-temperature reservoir. As we mention in the introduction section, we depart from this study and similar works in two aspects: (i) we build the reduced density matrix using an exact numerical treatment and (ii) we consider a more general model, including qubit–qubit interaction effects, with the motivation to consider a setup more relevant for quantum computation technologies. In this work we explore the entanglement dynamics by studying the time evolution of the system's state. It was recently proved that entanglement evolution, subjected to incoherent effects, could be resolved directly without the solution of the state dynamics [52].

4. Numerical results

We simulate the spin–boson dynamics in the P and Q branches separately using QUAPI [43], to obtain the population and coherences in each branch. With this at hand, we generate the 4×4 reduced density matrix $\rho_S(t)$, equation (17). The qubits degree of entanglement is calculated using equation (20). The entanglement characteristics discussed below were discovered earlier in related models, see, for example, [21, 26–30, 33, 34, 36, 54]. Our goal here is to obtain these effects within an exact treatment, as this could serve for testing the validity of approximate tools. Our general description assumes two thermal reservoirs: H_L, coupled to spin 1, and H_R, coupled to spin 2. These reservoirs are characterized by the spectral function $J_\nu(\omega) = \pi \sum_{k\in\nu} \lambda_k^2 \delta(\omega_k - \omega)$. Specifically, we simulate Ohmic baths, $J_\nu(\omega) = \frac{\pi K_\nu}{2} \omega\, \mathrm{e}^{-\omega/\omega_\mathrm{c}}$; ω_c is the cutoff frequency. The dimensionless prefactor K_ν is referred to as the Kondo parameter describing the strength of the system–bath interaction energy. In practice, our simulations were performed without the R reservoir, by taking $K_R = 0$. The reason for this choice is that in the spin–boson Hamiltonian (10) the inclusion of several reservoirs which are interacting in the same manner with the spins (the same functional form for B_L and B_R, up to a sign) simply amounts to an additive operation, reflecting a linear scaling of the Kondo parameter when more than one reservoir is incorporated. In what follows, we thus use the short notation $K \equiv K_L$, $K_R = 0$ and $T \equiv T_L$.

The energy parameters in the system are the qubit–qubit coupling, taken as $J = 1$, and the anisotropy parameters $\delta = 0.1$ and $\gamma = 0.5$. The qubits are assumed to be identical with $\epsilon_1 = \epsilon_2 \sim 0.1$–$0.5$. For the reservoir we take as a cutoff frequency $\omega_\mathrm{c} = 7.5$, and use temperatures in the range T=0.1–1. The Kondo parameter extends from the weak coupling limit ($K = 0.05$) to the strong–intermediate regime, $K = 0.8$, where convergence of QUAPI can be achieved. The following initial condition is utilized for the qubits subsystem:

$$\rho_S(0) = a\rho_Q(0) \oplus (1-a)\rho_P(0), \tag{22}$$

with $0 \leqslant a \leqslant 1$ and $\rho_{Q,P}(0)$ as the (maximally entangled) Bell states

$$\rho_Q(0) = \frac{1}{2}\begin{pmatrix} 1 & 1 \\ 1 & 1 \end{pmatrix}, \quad \rho_P(0) = \frac{1}{2}\begin{pmatrix} 1 & 1 \\ 1 & 1 \end{pmatrix}. \tag{23}$$

The concurrence (20) can be simplified if the following conditions are simultaneously satisfied: (i) $a \leqslant 1/2$ and (ii) $\epsilon_1 = \epsilon_2$. The latter condition, combined with the initial state ascribing identical weight to diagonal elements in the P subspace, implies that the populations in the P (single excitation) subspace are identical at all times, $(\rho_S)_{01,01} = (\rho_S)_{10,10} = \frac{1-a}{2}$.

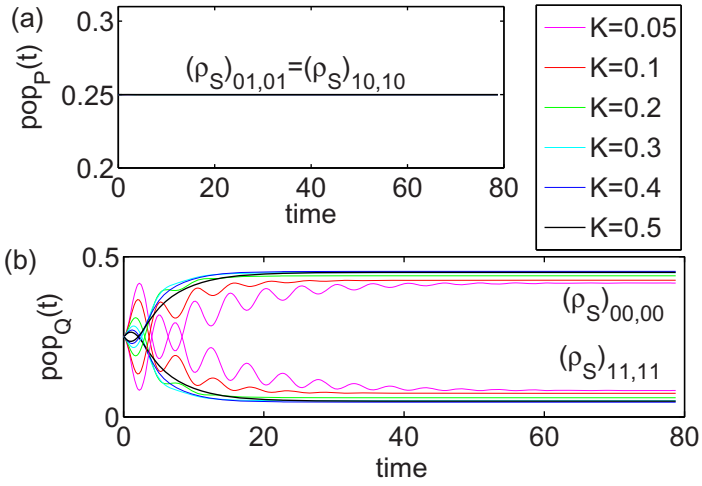

Figure 2. Population dynamics (a) in the single excitation subspace P and (b) in the zero and the double excitation subspace Q. We use the Bell states (22) as the initial density matrix with $a = 1/2$. $K = 0.05, 0.1, 0.2, 0.3, 0.4, 0.5$, bottom to top; the data at $K = 0.05$ are the most oscillatory. The other parameters are $\epsilon_1 = \epsilon_2 = 0.2$, $\delta = 0.1$, $\gamma = 0.5$, $T = 0.2$ and $J = 1$. QUAPI was used with a time step $\delta t = 0.25$ and a memory time $\tau_c = 9\delta t$. Convergence was verified by studying the behavior at different time steps δt and memory sizes τ_c.

Since $\sqrt{(\rho_S)_{00,00}(\rho_S)_{11,11}} \leqslant \frac{a}{2}$ at all times and the density matrix positivity condition demands that $|\rho_{i,j}|^2 \leqslant \rho_{i,i}\rho_{j,j}$, the off-diagonal terms are bounded by $|(\rho_S)_{11,00}| \leqslant \frac{a}{2}$. This implies that F_2 cannot be larger than zero at any instant for $a \leqslant 1/2$. The concurrence can then be simplified to

$$C_{a\leqslant\frac{1}{2}}(t) = \max(0, 2F_1). \tag{24}$$

This expression indicates that C is nonzero if the magnitude of the coherence in the P subspace is large, in comparison with the product of populations in the Q subspace. Thus, to understand the behavior of entanglement between the qubits one needs to follow the population and coherence dynamics in both subspaces. At the special point $a = 0$ the concurrence reduces to the simple form

$$C_{a=0}(t) = \max(|(\rho_S)_{01,10}|, 0), \tag{25}$$

which only depends on coherences behavior, a continuous function. As a result, concurrence sudden death is eliminated, indicating that this effect is directly linked to the inclusion of zero and double excitation components in the dynamics. It should be noted that such an entanglement, created between states with the same excitation number, is considered useless, since it is inaccessible experimentally due to particle (excitation number) conservation [53].

The qubits population behavior in time is displayed in figure 2, using $a = \frac{1}{2}$. The qubits have the same energy gap; thus in the P subspace the two states are degenerate and their population is identical at all times, independently of K. In contrast, in the Q subspace the energy difference between the states is significant, larger than the temperature, $T/2\epsilon < 1$; the tunneling element is given by $\gamma J = \frac{1}{2}$, with γ the anisotropy in the qubit–qubit coupling. In such a situation, we expect the steady-state population of the spin-up state to be significantly smaller

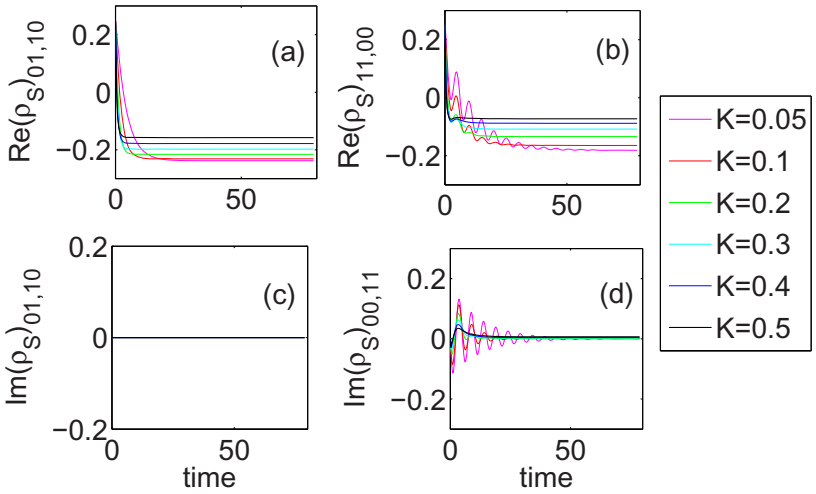

Figure 3. Real and imaginary parts of the coherences in the single excitation subspace P (a) and (c) and in the zero and double excitation subspace Q (b) and (d). The different lines were calculated with $K = 0.05, 0.1, 0.2, 0.3, 0.4, 0.5$. The parameters are the same as in figure 2.

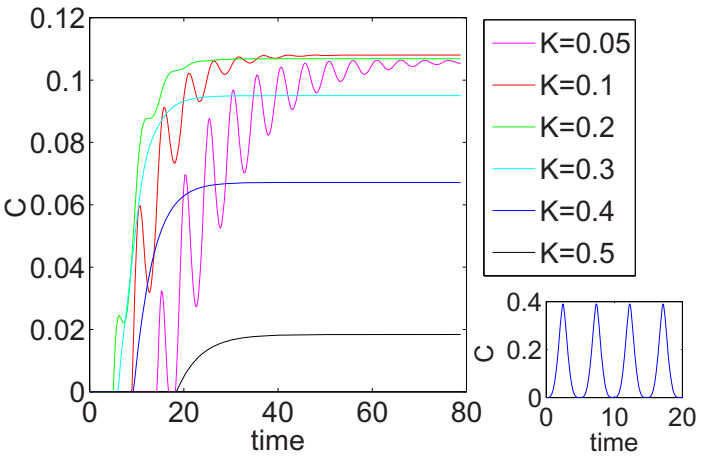

Figure 4. Concurrence between the two qubits as a function of time, manifesting a steady-state bath-induced entanglement generation. The different lines were calculated with $K = 0.05$, 0.1, 0.2, 0.3, 0.4, 0.5. Parameters are the same as in figure 2. Right panel: the concurrence dynamics in the absence of a thermal environment for the same set of qubit parameters.

than the ground state population, as indeed we observe in figure 2(b). An interesting observation is the phenomenon of population inversion between the zero and the double excitation states before the steady state sets in. This behavior occurs roughly up to a timescale that is inversely proportional to the Kondo parameter K, independent of the temperature. For the same set of parameters, figure 3 presents the coherence dynamics in the two subspaces. Generally, coherences are diminishing with an increase of K. Given the population and coherence dynamics, we display in figure 4 the concurrence, calculated using equation (24), manifesting

a rich dynamics. The following characteristics are of particular interest: (i) the birth time of the concurrence, (ii) its oscillations, (iii) the occurrence of sudden death and revival and (iv) the steady-state value. We now explain those properties.

Time-zero concurrence. The particular initial condition used here, $a = \frac{1}{2}$, results in $C(t = 0) = 0$. This is because while we are using maximally entangled states within each subspace as an initial condition, the entanglement between the two qubits themselves is zero initially, since all the relevant reduced density matrix elements, necessary for evaluating equation (24), are identical [50].

Delayed sudden birth. When $(\rho_S)_{00,00} \sim (\rho_S)_{11,11}$, a situation taking place at, and close to, the initial time, the concurrence should be zero, given the positivity condition that limits the value of off-diagonal elements. For small K, the time it takes the system to depart from its initial-equal population state is prolonged compared to a large-K case; thus, the concurrence birth time is delayed with respect to the large K behavior. Interestingly, the delay in the birth time does not extend linearly with K. Rather, the delay is significant for both $K = 0.05$ (weak system–bath coupling) and $K = 0.5$ (intermediate coupling), while it is shorter for in-between values, $K \sim 0.3$. The reason is that the delay time is a nontrivial function of both the time it takes the coherences to establish and the time it takes the population to significantly depart from the initial (equally populated) setup.

Oscillations. The oscillatory nature of C in time, best manifested for $K \leqslant 0.1$, reflects the Rabi-type oscillations of the diagonal elements $(\rho_S)_{00,00}$ and $(\rho_S)_{11,11}$. When these elements are similar in value, the concurrence drops, and even dies during a certain time interval, depending on the magnitude of the coherence at that time.

The steady-state value. If the two qubits are isolated from thermal effects ($K = 0$, the right panel of figure 4), the concurrence oscillations reflect the nature of the population and coherences dynamics, depicting Rabi oscillations. The qubits behavior under a dissipative thermal bath is notably distinct: since both population and coherences approach a constant at long time, the concurrence reaches a steady-state value as well. It predominantly reflects the magnitude of the coherence $(\rho_S)_{10,01}$ in the long-time limit since the population weakly depends on K at long time, see figure 2(b). Interestingly, for the present $a = \frac{1}{2}$ case the steady-state value of the concurrence is almost identical at weak system–bath coupling, $K = 0.05$–0.3. It significantly degrades around $K = 0.4$–0.5. Beyond that, it is identically zero.

Sudden death and revival. Based on figures 2–4, we can draw general conclusions regarding the process of entanglement sudden death. The effect is directly linked to the existence of population in the zero and double excitation states. If the dynamics within the Q space is eliminated altogether ($a = 0$), the concurrence is only controlled by the absolute value of the coherence $|(\rho_S)_{01,10}|$, equation (25). This quantity does not manifest an oscillatory behavior: under the present initial condition it starts at a large value, touches zero at a particular time and then grows again to a certain extent. (Under a different initial condition, e.g. $|(\rho_S)_{01,10}(0)| = 0$, the entanglement will systematically grow, up to the steady-state value.) In contrast, when the double excitation state is initially populated, oscillations between the states in the Q subspace largely occur if the system–bath coupling is weak. Then, the competition between the two terms in F_2, see equation (21), can result in disentanglement over a finite time interval.

Figure 5 displays the concurrence using different initial conditions, by playing with the parameter a. This modifies the weight of the zero and double excitation states in the dynamics. When $a = 0$ and $K = 0$ the entanglement is maximal ($C = 1$) at all times. For finite K, keeping $a = 0$, it dies at the particular point at which $|(\rho_S)_{01,10}| = 0$. Beyond that, it recovers to a

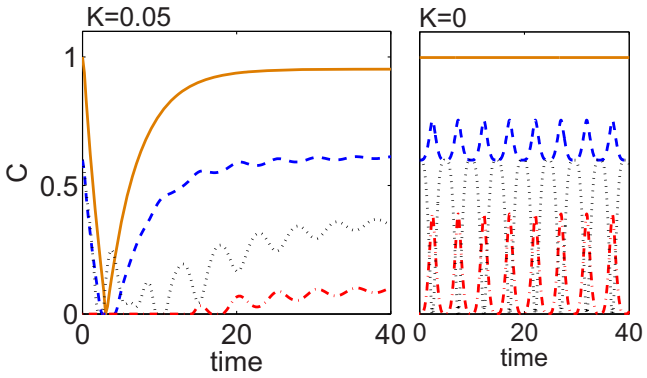

Figure 5. Concurrence between the two qubits as a function of time, using the Bell states (equation (22)) with $a = 0$ (full), $a = 0.2$ (dashed), $a = 0.5$ (dashed-dotted) and $a = 0.8$ (dotted). Left panel: $K = 0.05$; right panel: $K = 0$. Other parameters are the same as in figure 2.

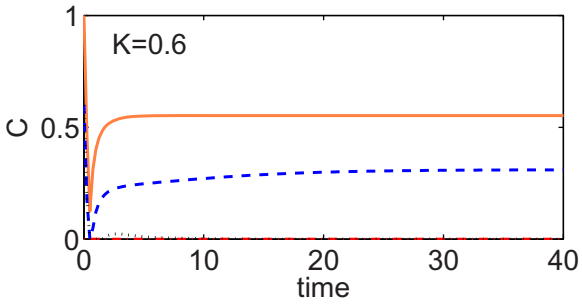

Figure 6. The same as figure 5 but at a strong system–bath coupling $K = 0.6$, $a = 0$ (full), $a = 0.2$ (dashed), $a = 0.5$ (dashed-dotted) and $a = 0.8$ (dotted).

value close to 1. When we include the Q states, e.g., by taking $a = 0.2$, we observe the effect of entanglement sudden death over a certain time interval. The duration of this interval grows when a is further increased up to $a \leqslant 1/2$. Beyond this point the coherence in the P subspace may dominate over the population in the Q subspace, resulting in a positive value for F_1, eliminating entanglement sudden death. The behavior at intermediate–strong system–bath coupling, $K = 0.6$, is included in figure 6, demonstrating that temporal oscillations are washed out. The dynamics at even larger K is similar in trend, with reduced concurrence value.

The role of temperature is displayed in figure 7. At high temperature the concurrence is zero. At intermediate values, $T < \epsilon$, we find that its sole effect is a shift-down of the qubit entanglement with increasing temperature. All other features (birth time, oscillation) stay intact. The simulation could not be performed at temperatures below $T \sim 0.1$ due to convergence issues in QUAPI.

We can readily study the concurrence under different initial conditions for the P and Q subspaces, not necessarily in the form of Bell states, as long as equation (14) is obeyed. In particular, using a diagonal state for the time-zero reduced density matrix, similar features to those discussed above were obtained.

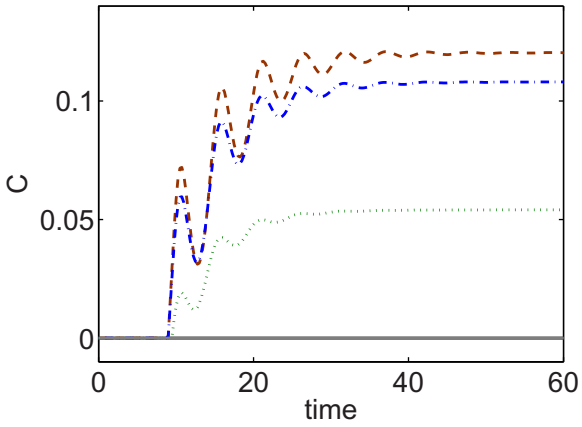

Figure 7. The role of the bath temperature on the concurrence evolution. $T = 0.1$ (dashed line), $T = 0.2$ (dashed-dotted line), $T = 0.4$ (dotted line) and $T = 0.6$ (full line). We use the Bell states (equation (22)) with $a = 0.5$ and $K = 0.1$. The other parameters are as in figure 2.

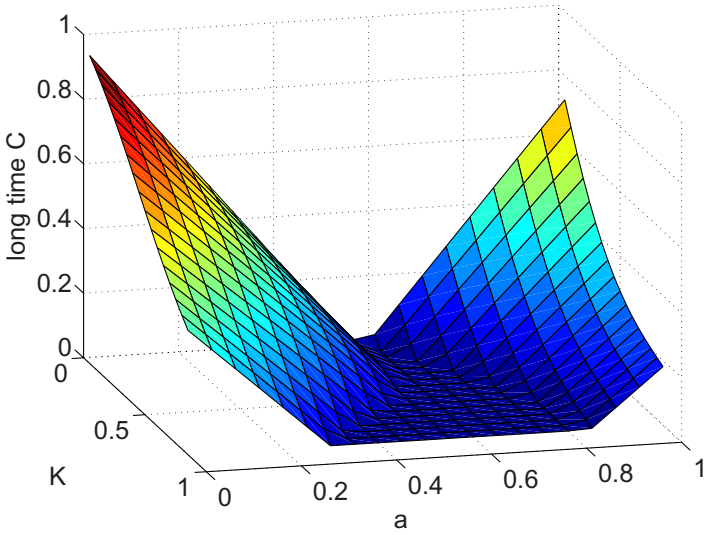

Figure 8. Concurrence at a long time, representing equilibrium behavior, for different initial states and system–bath coupling parameters. $T = 0.2$, $J = 1$, $\gamma = 0.5$, $\delta = 0.1$ and $\epsilon_1 = \epsilon_2 = 0.2$. The long-time limit was taken here as $t = 100$.

5. Universal features at a long time

The long-time behavior of the concurrence, representing the equilibrium limit, is displayed in figure 8 as a function of both K, the system–bath coupling parameter and the initial state preparation ratio a, see equation (22). We note that the concurrence can be significant in both the weak and strong coupling regimes, as long as the system evolves predominantly in either the P or Q subspaces. We now show that at weak coupling, $K \ll 1$, and at low temperatures, $T < J\gamma$, for a broad range of parameters (as we explain below), the following

general result holds:

$$C_{a<\frac{1}{2}}(t\to\infty)\sim 1-2a. \tag{26}$$

The important implication of this result is that to the lowest order in K the concurrence deviates from unity due to the occupation of the zero and doubly excited states in the system. This trend was observed before, e.g., in [54]. However, here, for the first time, it is justified analytically, based on the spin–boson model behavior [55]. We derive equation (26) by studying the long-time limit of F_1, as it dictates the concurrence when $a \leqslant \frac{1}{2}$, see equation (24). In the biased case, weak coupling theory (beyond the noninteracting blip approximation) provides [55]

$$\langle Q_z\rangle = (\rho_S)_{00,00}-(\rho_S)_{11,11}\sim a\frac{\epsilon}{\Delta_b}\tanh\left(\frac{\Delta_b}{T}\right), \tag{27}$$

in the thermodynamic limit. Here $\Delta_b^2=\epsilon^2+\Delta_{\rm eff}^2$, $\Delta_{\rm eff}$ is a nontrivial function of K, ω_c, and the bare tunneling element in the Q subspace, $J\gamma$. In the weak coupling limit we can write $\Delta_{\rm eff}\sim J\gamma$, thus $\Delta_b\sim\sqrt{\epsilon^2+J^2\gamma^2}$. Manipulating the polarization, we obtain the relevant term

$$\sqrt{(\rho_S)_{00,00}(\rho_S)_{11,11}}\sim\frac{a}{2}\sqrt{1-\left(\frac{\epsilon}{\Delta_b}\right)^2\tanh^2\left(\frac{\Delta_b}{T}\right)}. \tag{28}$$

The other element in F_1 is the coherence in the P subspace. In the long-time limit it satisfies [55]

$$|(\rho_S)_{01,10}|\sim\frac{1-a}{2}\frac{J}{\Omega}\tanh\left(\frac{\Omega}{T}\right), \tag{29}$$

where $\Omega^2=J^2+2J^2K\mu$; the proportionality factor obeys $\mu=\Re\psi(\mathrm{i}J/\pi T)-\ln(J/\pi T)$ with $\Re$ denoting the real part of ψ, the digamma function [55]. As expected, the equilibrium concurrence depends on the environmental temperature, leading to entanglement degradation at high T, as observed in figure 7. Considering the low temperature case, $T<J, J\gamma$, we note that the trigonometric term in both equations (28) and (29) is close to unity. If we further work in the region $\epsilon<J\gamma$, the square root expression in equation (28) gets close to 1. Under these broad conditions, the concurrence reduces to

$$\begin{aligned}C_{a<\frac{1}{2}}(t\to\infty)&\sim(1-a)\frac{1}{\sqrt{1+2\mu K}}-a\\&\sim 1-2a-\mu K(1-a).\end{aligned} \tag{30}$$

One should note that the K dependence is more subtle than the simple linear scale attained here, since the tunneling element J should be corrected by K in a nontrivial manner [55]. The simple result (30) provides us with some basic rules for building a long-time concurrence within the range of parameters mentioned above: (i) it decays linearly with the overall population placed in the Q (zero and double excitation) subspace; (ii) the reservoir temperature does not significantly affect it; and (iii) it does not depend on the qubit interaction energy. We note again that these observations are valid for $a<0.5$ when the temperature is low, $T<J, J\gamma$, energy gaps are small, $\epsilon<J\gamma$ and the system–bath coupling is weak, $K\ll 1$. When $a>0.5$, the concurrence is determined by the competition between F_1 and F_2, see equation (20). The numerics then suggests that $C_{a>\frac{1}{2}}(t\to\infty)\sim 2a-1$ holds, for similar energy parameters.

We conclude this section by emphasizing the implication of equation (26): one could *set* the steady-state entanglement in a *dissipative* system, by controlling the initial population in the P and Q subspaces.

6. Conclusions

Using exact numerical tools, we simulated the time evolution of two qubits immersed in thermal environments, considering a class of initial states for the subsystem. This task was achieved by reducing the two-qubit-bath model to two systems, whose dynamics could be readily followed separately. Using Wootters' formula for the concurrence, we quantified the degree of the qubits entanglement in time, exposing rich dynamics, including oscillations, delayed sudden birth, sudden death and revival. Specifically, we showed that the occurrence of entanglement sudden death can be traced down to the initial population of the zero and double excitation states. The steady-state behavior was discussed in the weak coupling limit.

Our results are significant for several reasons. (i) We exposed a general mapping between an anisotropic *XYZ* interacting two-qubit system embedded in a bath and a spin–boson-type model, allowing us to simulate the dynamics of the original model using a numerically exact method that was developed for studying the prominent spin–boson case. It should be noted that, in principle, exact simulations could be performed in the original two-qubit setup. However, such a simulation is significantly more costly than the method suggested here since the path-integral expression should follow all states of the subsystem. Using a path-integral approach, a direct n-step time evolution calculation should include $N = d^{2n}$ combinations, with d the dimensionality of the subsystem (the power of 2 in the exponent results from the need to perform forward and backward time evolution operations when following a density matrix dynamics). Thus, if $n = 10$ and $d = 2$, $N \sim 10^6$. In contrast, 10^{12} terms should be generated and summed up when $d = 4$ and $n = 10$. (ii) Based on our mapping scheme, we calculated the concurrence measure and demonstrated the essential role of the environment in generating a stationary entanglement between the (interacting) qubits. By engineering the environment and its interaction with the system, one could tune the degree of disentanglement in the system [56]. (iii) Since the method is in principle exact, simulations can be performed beyond the weak coupling limit. It is particularly interesting to note that intermediate dephasing strength ($K \sim 0.3$) does not substantially degrade the entanglement, compared to the weak coupling limit ($K \sim 0.05$), see figure 4. This endurance by the two-qubit system of dephasing effects makes it useful for quantum computing applications. Earlier studies in this field have mostly treated a simpler version of our model, ignoring the anisotropy in the qubit–qubit interaction energy, further utilizing perturbative treatments in the system–bath interacting term. To the best of our knowledge, our work is the first to calculate the concurrence exactly in the interacting qubit model beyond the weak system–bath coupling limit. This study could help in testing the validity of perturbative Markovian-based analytical results.

Future studies will focus on the dynamics of nonclassical correlations beyond the entanglement measure, evaluating quantum discord [57]. This could be done by relying on the X-form of the reduced density matrix [50, 51]. With this at hand, we plan to study the dynamics of classical and quantum correlations in the qubit system, specifically to investigate classical and quantum decoherence mechanisms and the possible transition between them [58]. The role of non-Markovian effects was not scrutinized in this work. While the method is exact and such effects are taken care of, with our choice of parameters (J, $J\gamma < \omega_c$) their contribution is practically small. It is important to explore the complementary region, J, $J\gamma \gtrsim \omega_c$, when non-Markovian effects are prominent. This case is particularly relevant in the context of energy transfer in biomolecules [19]. It is also interesting to extend the mapping scheme exposed here and treat other modular systems, e.g., a qubit coupled to a nano-resonator, or a dissipative qubit chain.

Acknowledgments

L-AW was supported by a CQIQC visitor grant, the Basque Government (Grant No. IT472-10), the Basque Country University UFI (Project No. 11/55-01-2013), and the Spanish MICINN (Project No. FIS2009-12773-C02-02). DS acknowledges support from an NSERC discovery grant. The research of CXY is supported by the Early Research Award of DS.

References

[1] Legget A J, Chakravarty S, Dorsey A T, Fisher M P A, Garg A and Zwerger W 1987 *Rev. Mod. Phys.* **59** 1
[2] Le Hur K 2008 *Ann Phys.* **323** 2208
[3] Segal D and Nitzan A 2005 *Phys. Rev. Lett.* **94** 034301
[4] Segal D 2006 *Phys. Rev.* B **73** 205415
[5] Loss D and DiVincenzo D P 1998 *Phys. Rev.* A **57** 120
[6] Orth P P, Roosen D, Hofstetter W and Le Hur K 2010 *Phys. Rev.* B **82** 144423
[7] Vierheilig C, Hausinger J and Grifoni M 2009 *Phys. Rev.* A **80** 052331
[8] Bloch I, Dalibard J and Zwerger W 2008 *Rev. Mod. Phys.* **80** 885
[9] Blatt R and Roos C F 2012 *Nature Phys.* **8** 277
[10] Fazio R and van der Zant H 2001 *Phys. Rep.* **355** 235
[11] Makhlin Y, Schön G and Shnirman A 2001 *Rev. Mod. Phys.* **73** 357
[12] Shnirman A, Schön G and Hermon Z 1997 *Phys. Rev. Lett.* **79** 2371
[13] Schoelkopf R J and Girvin S M 2008 *Nature* **451** 664
[14] Hanson R and Awschalom D D 2008 *Nature* **453** 1043
[15] Shulman M D, Dial O E, Harvey S P, Bluhm H, Umansky V and Yacoby A 2012 *Science* **336** 202
[16] Engel G S, Calhoun T R, Read E L, Ahn T-K, Mančal T, Cheng Y-C, Blankenship R E and Fleming G R 2007 *Nature* **446** 782
[17] Collini E, Wong C Y, Wilk K E, Curmi P M G, Brumer P and Scholes G D 2010 *Nature* **463** 644
[18] Gilmore J and McKenzie R H 2005 *J. Phys.: Condens. Matter* **17** 1735
[19] Gilmore J B and McKenzie R H 2006 *Chem. Phys. Lett.* **421** 266
[20] Eckel J, Reina J H and Thorwart M 2009 *New J. Phys.* **11** 085001
[21] Thorwart M, Eckel J, Reina J H, Nalbach P and Weiss S 2009 *Chem. Phys. Lett.* **478** 234
[22] Sarovar M, Ishizaki A, Fleming G R and Whaley K B 2010 *Nature Phys.* **6** 462
[23] Pachon L and Brumer P 2011 *J. Phys. Chem. Lett.* **2** 2728
[24] Hossein-Nejad H and Scholes G D 2010 *New J. Phys.* **12** 065045
[25] Horodecki R, Horodecki P, Horodecki M and Horodecki K 2009 *Rev. Mod. Phys.* **81** 865
[26] Yu T and Eberly J H 2004 *Phys. Rev. Lett.* **93** 140404
Yu T and Eberly J H 2006 *Phys. Rev. Lett.* **97** 140403
[27] Scheel S, Eisert J, Knight P L and Plenio M B 2003 *J. Mod. Opt.* **50** 881
[28] Benatti F, Floreanini R and Piani M 2003 *Phys. Rev. Lett.* **91** 070402
[29] Benatti F, Floreanini R and Marzolino U 2009 *Eur. Phys. Lett.* **88** 20011
Benatti F, Floreanini R and Marzolino U 2010 *Phys. Rev.* A **81** 012105
[30] Shan C-J, Cao S, Xue Z-Y and Zhu S-L 2012 *Chin. Phys. Lett.* **29** 040301
[31] Almeida M P, de Melo F, Hor-Meyll M, Salles A, Walborn S P, Souto P H Ribeiro and Davidovich L 2007 *Science* **316** 579
[32] Xu J-S, Li C-F, Gong M, Zou X-B, Shi C-H, Chen G and Guo G-C 2010 *Phys. Rev. Lett.* **104** 100502
[33] Ficek Z and Tanas R 2008 *Phys. Rev.* A **77** 054301
[34] Krauter H, Muschik C A, Jensen K, Wasilewski W, Petersen J M, Cirac J I and Polzik E S 2011 *Phys. Rev. Lett.* **107** 080503
[35] Petrucci F and Breuer H-P 2002 *The Theory of Open Quantum Systems* (Oxford: Oxford University Press)

[36] Al-Qasimi A and James D F V 2008 *Phys. Rev.* A **77** 012117
[37] Bellomo B, Lo Franco R and Compagno G 2007 *Phys. Rev. Lett.* **99** 160502
[38] Ekert A K 1991 *Phys. Rev. Lett.* **67** 661
[39] Dube M and Stamp P C E 1998 *Int. J. Mod. Phys.* B **12** 1191
[40] Governale M, Grifoni M and Schön G 2001 *Chem. Phys.* **268** 273
[41] Ahn D, Oh J H, Kimm K and Hwang S W 2000 *Phys. Rev.* A **61** 052310
[42] Thorwart M and Hänggi P 2001 *Phys. Rev.* A **65** 012309
[43] Makarov D E and Makri N 1994 *Chem. Phys. Lett.* **221** 482
Makri N and Makarov D E 1995 *J. Chem. Phys.* **102** 4600
Makri N and Makarov D E 1995 *J. Chem. Phys.* **102** 4611
Makri N 1995 *J. Math. Phys.* **36** 2430
[44] Golosov A A, Friesner R A and Pechukas P 1999 *J. Chem. Phys.* **110** 138
[45] Wootters W K 1998 *Phys. Rev. Lett.* **80** 2245
[46] Mahan G D 2000 *Many-Particle Physics* (New York: Plenum)
[47] Reichman D, Silbey R J and Suarez A 1996 *J. Chem. Phys.* **105** 10500
[48] Wu L-A and Lidar D A 2002 *J. Math. Phys.* **43** 4506
[49] Wu L-A and Lidar D A 2003 *Phys. Rev. Lett.* **91** 097904
[50] Ali M, Rau A R P and Alber G 2010 *Phys. Rev.* A **81** 042105
[51] Li B, Wang Z-X and Fei S-M 2011 *Phys. Rev.* A **83** 022321
[52] Konard T, De Melo F, Tiersch M, Kasztelan C, Aragão A and Buchleitner A 2008 *Nature Phys.* **4** 99
[53] Beenakker C W J 2006 *Proc. Int. School of Physics E Fermi* vol 162 ed G Casati, D L Shepelyansky, P Zoller and G Benenti (Amsterdam: IOS) pp 307–47
[54] Ikram M, Li F-L and Zubairy M S 2007 *Phys. Rev.* A **75** 062336
[55] Weiss U 1993 *Quantum Dissipative Systems* (Singapore: World Scientific)
[56] Verstraete F, Wolf M M and Cirac J I 2009 *Nature Phys.* **5** 633
[57] Ollivier H and Zurek W H 2001 *Phys. Rev. Lett.* **88** 017901
[58] Mazzola L, Piilo J and Maniscalco S 2010 *Phys. Rev. Lett.* **104** 200401